Toxicology and Applied Pharmacology 334 (2017) 8–17

Contents lists available at ScienceDirect

Toxicology and Applied Pharmacology

journal homepage: www.elsevier.com/locate/taap

Neuromuscular paralysis by the basic phospholipase A_2 subunit of crotoxin from *Crotalus durissus terrificus* snake venom needs its acid chaperone to concurrently inhibit acetylcholine release and produce muscle blockage

Walter L.G. Cavalcante[a,b,d,1], José B. Noronha-Matos[b,c,1], Maria A. Timóteo[b,c], Marcos R.M. Fontes[d], Márcia Gallacci[e], Paulo Correia-de-Sá[b,c,*]

[a] Departamento de Farmacologia, Instituto de Ciências Biológicas, UFMG, Av. Antônio Carlos, 6627 Belo Horizonte, Brazil
[b] Laboratório de Farmacologia e Neurobiologia, Instituto de Ciências Biomédicas Abel Salazar - Universidade do Porto (ICBAS-UP), R. Jorge Viterbo Ferreira, 228, 4050-313 Porto, Portugal
[c] Center for Drug Discovery and Innovative Medicines (MedInUP), Instituto de Ciências Biomédicas Abel Salazar - Universidade do Porto (ICBAS-UP), R. Jorge Viterbo Ferreira, 228, 4050-313 Porto, Portugal
[d] Departamento de Física e Biofísica, Instituto de Biociências, UNESP, Distrito de Rubião Jr., Botucatu, 18618-970, São Paulo, Brazil
[e] Departamento de Farmacologia, Instituto de Biociências, UNESP, Distrito de Rubião Jr., Botucatu, 18618-970, São Paulo, Brazil

ARTICLE INFO

Keywords:
Crotalus durissus terrificus
Crotalinea Snake Venom
Phospholipase A_2
[^{3}H]-Acetylcholine Release
Real-time transmitter exocytosis
Neuromuscular transmission

ABSTRACT

Background and purpose: Crotoxin (CTX), a heterodimeric phospholipase A_2 (PLA_2) neurotoxin from *Crotalus durissus terrificus* snake venom, promotes irreversible blockade of neuromuscular transmission. Indirect electrophysiological evidence suggests that CTX exerts a primary inhibitory action on transmitter exocytosis, yet contribution of a postsynaptic action of the toxin resulting from nicotinic receptor desensitization cannot be excluded. Here, we examined the blocking effect of CTX on nerve-evoked transmitter release measured directly using radioisotope neurochemistry and video microscopy with the FM4-64 fluorescent dye.

Experimental approach: Experiments were conducted using mice phrenic-diaphragm preparations. Real-time fluorescence video microscopy and liquid scintillation spectrometry techniques were used to detect transmitter exocytosis and nerve-evoked [^{3}H]-acetylcholine ([^{3}H]ACh) release, respectively. Nerve-evoked myographic recordings were also carried out for comparison purposes.

Key results: Both CTX (5 μg/mL) and its basic PLA_2 subunit (CB, 20 μg/mL) had biphasic effects on nerve-evoked transmitter exocytosis characterized by a transient initial facilitation followed by a sustained decay. CTX and CB reduced nerve-evoked [^{3}H]ACh release by 60% and 69%, respectively, but only the heterodimer, CTX, decreased the amplitude of nerve-evoked muscle twitches.

Conclusion and implications: Data show that CTX exerts a presynaptic inhibitory action on ACh release that is highly dependent on its intrinsic PLA_2 activity. Given the high safety margin of the neuromuscular transmission, one may argue that the presynaptic block caused by the toxin is not enough to produce muscle paralysis unless a concurrent postsynaptic inhibitory action is also exerted by the CTX heterodimer.

1. Introduction

Crotoxin (CTX), the primary component of *Crotalus durissus terrificus* (South American rattlesnake) venom (Slotta and Fraenkel-Conrat, 1938), is a potent neurotoxin that induces peripheral respiratory paralysis due to the blockage of neuromuscular transmission (Brazil et al., 1966; Breithaupt et al., 1974). Structurally, CTX is a heterodimeric protein composed by the non-covalent association of a basic subunit (CB), which exhibits phospholipase A_2 (PLA_2) activity, and an acidic subunit (CA) that lacks enzymatic activity (Hendon and Fraenkel-Conrat, 1971; Breithaupt et al., 1974; Breithaupt, 1976; Marchi-Salvador et al., 2008; Faure et al., 2011; Fernandes et al., 2017). Alone,

Abbreviations: [^{3}H]-ACh, [^{3}H]-acetylcholine; α-BTX, α-bungarotoxin; CA, acidic subunit; CB, basic PLA_2 subunit; CTX, crotoxin; EPP, endplate potentials; FM4-64, *N*-(3-triethylammoniumpropyl)-4-(6-(4-(diethylamino)phenyl) hexatrienyl) pyridinium dibromide; HPLC, high performance liquid chromatography; PLA_2, phospholipase A_2; ROI, region of interest; RP, reverse phase

* Corresponding author at: Laboratório de Farmacologia e Neurobiologia/MedInUP, Instituto de Ciências Biomédicas de Abel Salazar (ICBAS) – Universidade do Porto (UP), R. Jorge Viterbo Ferreira, 228, 4050-313 Porto, Portugal.
E-mail address: farmacol@icbas.up.pt (P. Correia-de-Sá).
[1] These authors contributed equally to this work.

http://dx.doi.org/10.1016/j.taap.2017.08.021
Received 20 June 2017; Received in revised form 10 August 2017; Accepted 30 August 2017
Available online 01 September 2017
0041-008X/

CB is slightly toxic and CA is non-toxic, but both subunits act synergistically to achieve significant toxicity; CA acts as a chaperone of CB, thus preventing its binding to non-specific sites (Bon et al., 1979). Several CA and CB isoforms have been isolated and characterized, showing that CTX is a mixture of different molecules derived from the combination of distinct subunit isoforms (Faure et al., 1994).

The neurotoxic effect of CTX has been mainly attributed to a presynaptic action leading to inhibition of acetylcholine release from stimulated motor nerve terminals. This hypothesis is based on a series of electrophysiological studies demonstrating that CTX depresses the quantal content of endplate potentials (EPPs) in both mammalian and amphibian neuromuscular preparations (Brazil and Excell, 1971; Chang and Lee, 1977; Hawgood and Smith, 1977; Hawgood and Santana de Sa, 1979). Although these findings are unequivocal evidences of an inhibitory presynaptic action, they were obtained under experimental conditions designed to reduce the safety margin of the neuromuscular transmission that are required to measure the amplitude of motor endplate potentials in skeletal muscle fibres with sharp intracellular microelectrodes. These conditions imply the presence of low Ca^{2+}/high Mg^{2+} concentrations in the incubation fluid or the blockage of muscle-type nicotinic receptors with D-tubocurarine that, on their own, decrease the probability of transmitter release and the sensitivity of the post-synaptic membrane, respectively. Notwithstanding this, it has been hypothesized that CTX may contribute to flaccid skeletal muscle paralysis by causing postsynaptic nicotinic receptors desensitization (Brazil et al., 2000). The postsynaptic nature of this effect has been confirmed because CTX is capable of depressing acetylcholine responses on rat denervated hemidiaphragm preparations (Brazil, 1966; Brazil et al., 1966). Later on, experiments performed with *Electrophorus electricus* electroplaques and excitable microsacs prepared from *Torpedo marmorata* electric organ preloaded with $^{22}NaCl$ showed that CTX blocks depolarization and $^{22}Na^{+}$ efflux caused by cholinoceptor agonists, respectively. Together, these results suggest that the CTX heterodimer promotes stabilization of nicotinic receptors in the desensitized state when administered at low concentrations, supporting a role for CTX at a recognition site on the postsynaptic membrane (Bon et al., 1979; Brazil et al., 2000).

Despite the neurotoxicity, several studies have pointing towards other biological activities of CTX that have potential pharmacological value such as immunomodulatory, anti-nociceptive, anti-inflammatory, anti-tumoral and anti-microbial activities (Sampaio et al., 2010; Favoretto et al., 2011; Ye et al., 2011; Wang et al., 2012; He et al., 2013; Han et al., 2014; Almeida et al., 2015; Brigatte et al., 2016; Faure et al., 2016). Thus, a more complete understanding of the neurotoxic action of CTX is relevant not only to improve the treatment of envenomation, but also to enable the biotechnological use of this toxin or new drugs derived from this protein. This contention led us to examine the presynaptic action of CTX and its CB subunit in more physiological conditions of transmitter release and without the influence of post-synaptic neuromuscular block inherent to electrophysiological techniques. To this end, we used phrenic nerve-hemidiaphragm preparations of mice to directly assess transmitter release from stimulated nerve terminals using radioisotope neurochemistry and real-time video microscopy with the FM4-64 fluorescent dye (Correia-de-Sá et al., 2013; Noronha-Matos et al., 2011; Noronha-Matos and Correia-de-Sá, 2014). For comparison purposes, we also performed nerve-evoked myographic recordings under the same experimental conditions to assess the significance of the presynaptic action of CTX and its CB subunit to establishment of the neuromuscular paralysis.

2. Materials and methods

2.1. Toxins and drugs

CTX and its basic subunit (CB) were purified from *Crotalus durissus terrificus* venom by molecular exclusion and reverse phase (RP) high performance liquid chromatography (HPLC) (ÄKTA Purifier system, GE Healthcare), respectively. The procedure used to fractionate CTX and CB subunit was similar to previous studies (Oliveira et al., 2002; Hernandez-Oliveira et al., 2005).

Radiolabeled [methyl-^{3}H] choline chloride (ethanol solution, 80.6 Ci $mmol^{-1}$) and the scintillation cocktail (Insta-gel Plus) were obtained from Perkin Elmer (Boston, USA). *N*-(3-triethylammoniumpropyl)-4-(6-(4-(diethylamino)phenyl) hexatrienyl) pyridinium dibromide (FM4-64) and tetramethylrhodamine-conjugated α-bungarotoxin were purchased from ThermoFisher Scientific (Waltham, MA, USA). FM4-64 and tetramethylrhodamine-conjugated α-BTX were made up in dimethylsulphoxide; α-bungarotoxin (α-BTX) used in vitro to prevent muscle fiber contractions was made up in 400 μM stock solution in water. All stock solutions were stored as frozen aliquots at − 20 °C. Dilutions of these stock solutions were made daily and appropriate solvent controls were done. No statistically significant differences between control experiments, made in the absence or in the presence of the solvents at the maximal concentrations used, were observed. All other reagents were of analytical grade.

2.2. Animals

Mice (CD-1® IGS) were purchased from Charles River Laboratories (Barcelona, Spain). We used sexually mature adult mice (8–10 weeks old) of either sex with average weights of 37 ± 1 g and 31 ± 1 g concerning males and females, respectively; no gender differences were detected in preliminary experiments performed to test the sensitivity of in vitro neuromuscular transmission to CTX and its CB subunit. Animals were kept at a constant temperature (21 °C) and a regular light (06:30–19:30 h) - dark (19:30–06:30 h) cycle with food and water ad libitum. On the day of the experiment, the animals were killed after stunning followed by exsanguination. Animal handling and experiments followed the guidelines defined by the European Communities Council Directive (86/609/EEC) and in accordance with the guidelines prepared by the Committee on Care and Use of Laboratory Animal Resources (National Research Council, USA). All animal studies comply with the ARRIVE guidelines.

2.3. Myographic recordings

Phrenic nerve–diaphragm muscle preparations were isolated and mounted vertically in a conventional isolated organ bath chamber containing 15 mL of Ringer solution (mM): NaCl, 135; KCl, 5; $MgCl_2$, 1; $CaCl_2$, 2; $NaHCO_3$, 15; Na_2HPO_4, 1; glucose, 11. This solution was continuously gassed with 95% O_2 and 5% CO_2. The preparation was attached to an isometric force transducer (Grass, FT03, Quincy, MA, USA) for recording the twitch tension. The transducer signal output was amplified and recorded on a computer via a transducer signal conditioner (Gould, 13-6615-50, USA) with an AcquireLab Data Acquisition System (Gould, USA). Indirect contractions were evoked by supramaximal intensity pulses delivered via a Grass S88 K (Quincy, MA, USA) stimulator and applied to the phrenic nerve by means of a suction electrode. The preparations were equilibrated for 45 min at a resting tension of 50 mN. During equilibrium, the phrenic nerve was stimulated with supramaximal rectangular pulses (0.4 ms duration, 0.2 Hz frequency) and stopped at the end of the period. After the equilibrium, muscle twitches had an average amplitude of 20.4 ± 2.0 mM (n = 35). Toxins were tested under two different experimental conditions: 1) to evaluate the blocking activity of CTX or CB on nerve-evoked muscle twitches delivered at 0.2 Hz frequency, each toxin was applied to the bathing solution and their effects measured for 120 min; 2) the blocking effects of CTX and CB were also tested on muscle contractions evoked by stimulating the phrenic nerve three times with 5-Hz frequency trains of 150 s each (0.4 ms pulse duration) starting at the 12th (S_1), 39th (S_2) and 75th (S_3) min after the end of the equilibrium (zero time). CTX (5 μg/mL) or CB (20 μg/mL) were added 21 min after the

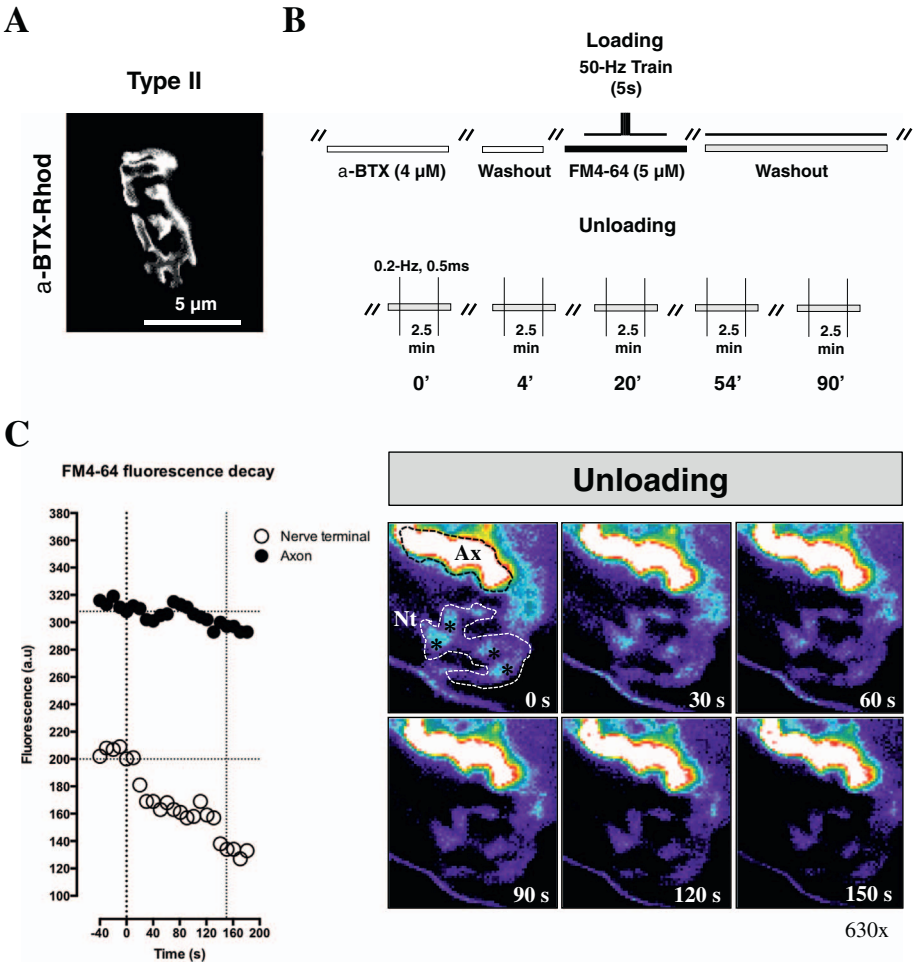

Fig. 1. Nerve-evoked transmitter exocytosis measured by video-microscopy using the FM4-64 fluorescent dye on mice phrenic nerve-hemidiaphragm preparations. (A) Show is an epifluorescence micrograph of a typical type II motor endplate labelled with tetramethylrhodamine-conjugated α-bungarotoxin (α-BTX-Rhod). (B) Schematic diagram of the loading and unloading protocol with FM4-64 fluorescent dye; for details, see Materials and Methods. (C) Representative graph of the FM4-64 fluorescence decay during electrical stimulation of the phrenic nerve (0.2 Hz, 0.5 ms, 30 pulses) in a control experiment. Fluorescence decay in arbitrary units (a.u.) expressed as a percentage of maximal loading considering that 100% is the fluorescence intensity at zero time verified at the nerve terminal (region of interest) and at the axon (negative internal control). Vertical dashed lines represent the beginning and the end of the stimulation period. Right hand-side panels represent FM4-64 fluorescence intensity changes during unloading from a typical type II nerve terminal (Nt) and axon (Ax). Images were taken at the indicated times just before, during and after phrenic nerve stimulation using a 63 ×/0.90 n.a. water-immersion objective lens (Achroplan; Zeiss). Loaded nerve terminals with the FM4-64 dye show typical hot spots (*), which are preferred sites of exocytosis that co-localize with fast delivery pool of vesicles (see Noronha-Matos et al., 2011). Zoom was 630 ×.

end of the equilibrium period (zero time) and were present up to the end of the experiment. Changes in the ratio between indirectly evoked twitches during S_2 (Control: 18.7 ± 2.9 mN, n = 4) or S_3 (Control: 18.4 ± 2.8 mN, n = 4) compared to that observed in the absence of CTX or CB (S_1; Control: 19.6 ± 3.3 mN, n = 4), were taken as a measure of the toxin effect.

2.4. Evoked [^{3}H]ACh release

The experiments were performed using either the left or the right phrenic nerve-hemidiaphragm preparations (4–6 mm width). The procedures used for labelling the preparations and measuring evoked [^{3}H]ACh release were used as previously described (Wessler and Kilbinger, 1986; Correia-de-Sá et al., 1991, 1996, 2013; Noronha-Matos et al., 2011; Oliveira et al., 2015) with minor modifications. Briefly, the preparations were superfused (3 mL/min) in 3-mL organ baths at 37 °C with Tyrode's solution containing (mM) NaC1 137, KC1 2.7, $CaC1_2$ 1.8, $MgC1_2$ 1, NaH_2PO_4 0.4, $NaHCO_3$ 11.9, glucose 11.2 and choline 0.001, which was continuously gassed with 95% O_2 and 5% CO_2. After a 30 min of equilibration period, the perfusion was stopped and the nerve endings were labelled during 40 min with 1 µM [^{3}H]choline (specific activity 2.5 µCi/nmol) under electrical stimulation at 1 Hz with supramaximal rectangular pulses of 15 V and 0.4 ms duration. After the end of the labelling period, the preparations were again superfused (15 mL/min) and the nerve stimulation stopped. From this time onwards, hemicholinium-3 (10 µM) was present to prevent uptake of choline. After a 56-min period of washout, the perfusion was stopped, and 1.4-mL bath samples were collected every 3 min by emptying and refilling the organ bath with the solution in use. Aliquots (400 µL) of the incubation medium were added to 3.5 mL of Insta-gel Plus scintillator. Tritium content of the samples was measured by liquid scintillation spectrometry (Perkin Elmer TriCarb 2900TR; % tritium efficiency: 58 ± 2%) after appropriate background subtraction, which did not exceed 5% of the tritium content of the samples. The radioactivity was expressed as disintegrations per minute per gram of wet weight of the tissue (DPM/g), determined at the end of the experiment. After the loading and washout periods, the preparation contained (4867 ± 156) × 10^3 DPM/g and the resting release was (123 ± 14) × 10^3 DPM/g (n = 16). The fractional release was calculated to be 2.05 ± 0.08% of the radioactivity present in the tissue at the first collected sample (see e.g. Oliveira et al., 2015).

The phrenic nerve was stimulated with an extracellular glass-platinum suction electrode placed near the first division branch of the nerve trunk, to avoid direct contact with muscle fibres. 750 supramaximal-intensity rectangular pulses (0.04 ms duration, 8 mA) were delivered at 5-Hz frequency. Pulses were generated by a stimulator (Grass S48; Quincy, MA, USA) coupled to a stimulus isolation unit (Grass SIU5, USA) operating in current constant mode.

The experimental protocol used to determine [^{3}H]ACh release was similar to the protocol 2 used in myographic recordings (see above). That is, [^{3}H]ACh release was evoked by three periods of electrical stimulation of the phrenic nerve, starting at the 12th (S_1), 39th (S_2) and 75th (S_3) min after the end of washout (zero time). The evoked fractional release of [^{3}H]ACh was calculated by subtracting baseline from the total fractional release during the stimulation period (Correia-de-Sá et al., 1991; Oliveira et al., 2015), i.e. the ratio between the evoked [^{3}H]ACh release during S_2 or S_3 and the evoked [^{3}H]ACh release during S_1. CTX (5 µg/mL) or CB (20 µg/mL) were added 21 min after the end

of washout (zero time) and were present up to the end of the experiment. The changes in the ratio between the evoked [^{3}H]ACh release during the stimulation periods S_2 or S_3 relative to that observed in control situations (in the absence of test drugs S_1) were taken as a measure of the toxin effect.

2.5. Real-time video-microscopy using the FM4-64 fluorescent dye as a measure of transmitter exocytosis

The procedures used for labelling nerve terminals and measuring real-time exocytosis were those previously described (Noronha-Matos et al., 2011; Correia-de-Sá et al., 2013; Noronha-Matos and Correia-de-Sá, 2014) with minor modifications. We used the FM4-64 fluorescent dye, focusing our attention on real-time nerve-evoked transmitter exocytosis from a subset of synaptic vesicles (defined as the high-probability release pool or fast destaining pool), which are preferentially loaded following the first 5 s (250 action potentials) at 50 Hz (Perissinotti et al., 2008; Noronha-Matos et al., 2011; Correia-de-Sá et al., 2013). The preparations were mounted on the stage of an upright epifluorescence microscope (Zeiss Axiophot, Oberkochen, Germany) and thereafter incubated as for the release of [^{3}H]ACh. After a 30 min equilibration period, phrenic nerve-hemidiaphragm preparations were incubated with α-BTX (4 μM, during 15–20 min) to prevent nerve-evoked muscle fiber contractions that would otherwise complicate the analysis of fluorescence signals under the microscope (Fig. 1B). α-BTX irreversibly blocks muscle-type nicotinic ACh receptors containing α1 subunits with no action on the nicotinic receptors present on motor nerve terminals (Plomp et al., 1992; Faria et al., 2003). After a 10-min incubation period with FM4-64 (5 μM) made up in Tyrode's solution, loading of synaptic vesicles was achieved by stimulating the phrenic nerve trunk with 250 pulses of supramaximal intensity (0.04 ms duration, 8 mA) applied at a frequency of 50 Hz, followed by an additional 10-min period of rest with the dye. To remove the excess of the dye from the incubation fluid, a washout period was performed during 30 min (Fig. 1B). Fluorescence images were acquired using a 63 ×/0.90 n.a. water-immersion objective lens (Achroplan; Zeiss). After the equilibration period, CTX (5 μg/mL) or CB (20 μg/mL) were added to the incubation medium and remained in contact with preparations through a closed automatic perfusion system (ValveLink8.2, Digitimer, Welwyn Garden City, UK) connected to a fast solution heating device (TC-344B, Harvard Apparatus, March-Hugstetten, Germany). The phrenic nerve was stimulated (0.2 Hz, 0.5 ms duration, 30 pulses) immediately before administration of CTX or CB and subsequently at 4, 20, 54 and 90 min. Pulses were generated by a Grass S48 (Quincy, MA, USA) stimulator.

Fluorescence excitation light came from a XBO 75 W Xenon arc lamp via a BP 546/12 nm excitation filter; fluorescence emission was filtered with a LP 590 nm filter. Images were acquired in the real-time mode with a high-resolution cooled CCD camera (CoolSnap HQ, Roper Scientific Photometrics, Tucson, AZ, USA) connected to a computer running a digital image acquisition software (MetaFluor 6.3; Molecular Devices Inc., Sunnyvale, CA, USA). Exposure time was adjusted between 150 and 250 ms (binning was adjusted to 2–3 and gain to 1–2). Regions of interest (terminal areas) of each motor endplate were manually outlined and the average intensity of the pixels inside this area was calculated. Background fluorescence was estimated from an outlined region surrounding the motor endplate and from fluorescence of non-stimulated motor endplate, which was then subtracted from the average fluorescence measured at the interest motor endplate. The corrected nerve terminal fluorescence values measured (in arbitrary units, a.u.) before each stimulation period applied 0, 4, 20, 54 and 90 min after washing out the dye (Fig. 1B) decayed from 119 ± 32, 101 ± 29, 72 ± 21, 62 ± 14 to 40 ± 9, respectively. To facilitate comparisons between different preparations, fluorescence was measured as the percentage of the maximum dye load. Absolute fluorescence measurements were converted to a percentage of the maximum fluorescence detected after staining. The following equations were used:

$$R(t) = \frac{F_{ter}(t) - F_{bg}(t)}{F_{ax}(t) - F_{bg}(t)} \quad (1)$$

R(t) was obtained dividing the terminal fluorescence (F_{ter}) by the axon's fluorescence (F_{ax}) at time t; the unspecific fluorescence (F_{bg}, background) was subtracted for each point; during electrical stimulation of the phrenic nerve, a significant decay of FM4-64 fluorescence was observed from loaded synaptic vesicles inside nerve terminals, but not in non-vesicular areas, like axons (see Fig. 1C).

$$\%F(t) = 100 \times \frac{R(t)}{R^{MAX}} \quad (2)$$

$F(t)$ is the absolute fluorescence at time t; R^{MAX} is the absolute fluorescence after maximum loading. Under these experimental conditions, nerve-evoked FM4-64 intensity decay reflects synaptic vesicle exocytosis at the nerve terminal (see Betz et al., 1992; Perissinotti et al., 2008; Noronha-Matos et al., 2011; Correia-de-Sá et al., 2013). For further details on the technique, please report to Noronha-Matos and Correia-de-Sá (2014).

2.6. Fluorescence labelling of motor endplates with tetramethylrhodamine-conjugated α-BTX

In order to identify regions of interest (ROI, nerve terminals), motor endplates were labelled with tetramethylrhodamine-conjugated α-BTX (1.25 μM) for 30 min and then washed in Tyrode's solution. Observations were performed as previously described (Noronha-Matos et al., 2011). The morphology of motor endplates subtypes recognized by the labelling muscle-type nicotinic receptors were evaluated (see e.g. Prakash et al., 1996). We focused on type II motor endplates (Fig. 1A), since these are more easily identified due to their larger dimension (14 ± 1 μm^2, versus 10 ± 2 μm^2 for type I motor endplates).

2.7. Statistics

The data are expressed as mean ± SEM from an n number of experiments. Statistical analysis of data was carried out, using: 1) one-way or two-way ANOVA, Bonferroni's multiple comparison test; 2) multiple t-test, assuming same scatter (SD) per point, Bonferroni-Dunn method. Values of $p < 0.05$ were considered to represent significant differences.

3. Results

3.1. Time course of the neuromuscular block produced by CTX and CB during stimulation of the phrenic nerve with 0.2-Hz frequency

CTX caused a time- and concentration-dependent blockade of indirectly evoked twitches (Fig. 2A). On average, the time required for CTX to reduce the amplitude of nerve-evoked twitches by a half ($t_{1/2}$) was > 90 min when CTX was applied at 1 μg/mL (n = 7), but this time decreased to 54.34 ± 3.40 min (n = 5), 41.15 ± 2.56 min (n = 8) and 43.90 ± 5.20 min (n = 4) when concentrations of 5, 10 and 20 μg/mL were used, respectively. Fig. 2A also shows that CTX (5 μg/mL) caused a slight increase in the amplitude of nerve-evoked muscle twitches during the first 15 min of application, which was followed by a progressive decline towards complete muscle paralysis verified 120 min after starting toxin incubation; this gradual decline became significant ($p < 0.01$) 45 min after exposure to the toxin (Fig. 2A). In order to explore the biphasic effect CTX, the 5 μg/mL concentration was selected to use in subsequent experiments. This concentration is 3–6 fold higher the estimated blood concentrations (0.87–1.40 μg/mL) achieved by intravenous administration of CTX at concentrations near the LD_{50} (52–82 μg/Kg) to cause death by neuromuscular paralysis (Brazil et al.,

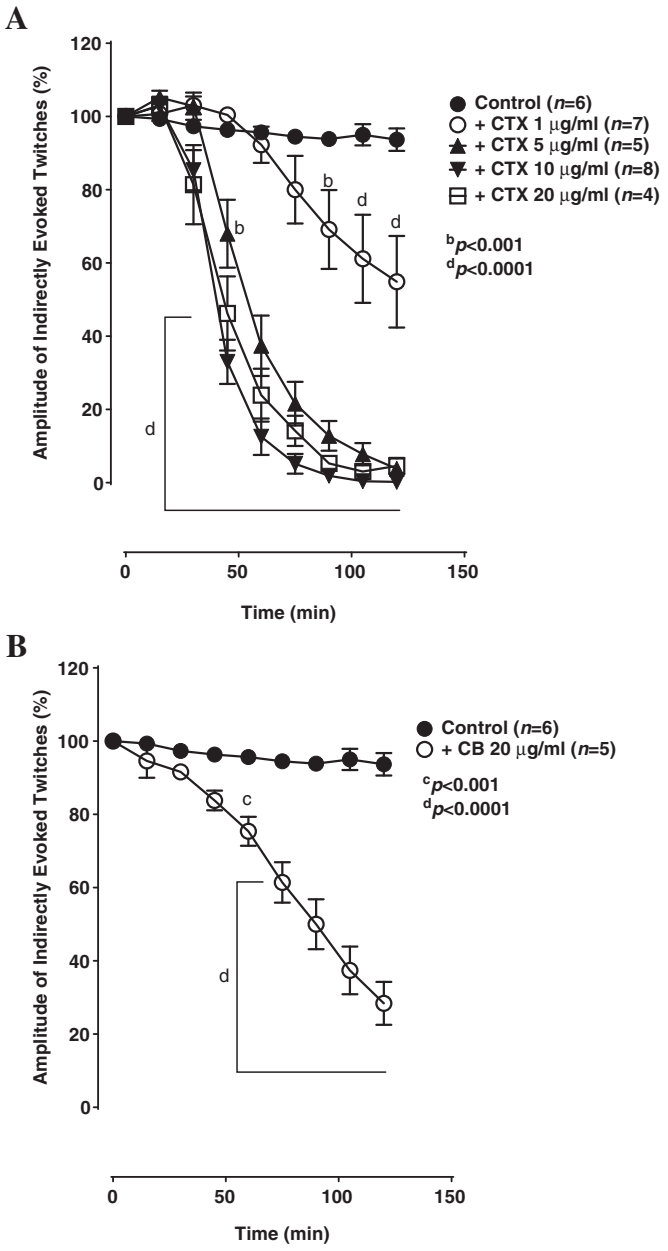

Fig. 2. Effects of CTX (A) and its basic subunit, CB (B), on diaphragm muscle twitches triggered by stimulation of the phrenic nerve with supramaximal intensity pulses delivered at 0.2 Hz frequency. Ordinates represent the percentage amplitude of twitches relative to the initial control situation. Abscissa indicates the time (min) after CTX (1, 5, 10 and 20 μg/mL) or CB (20 μg/mL) application to the organ bath. The vertical bars represent ± SEM. $^{b}p < 0.01$, $^{c}p < 0.001$ and $^{d}p < 0.0001$ (two-way ANOVA followed by Bonferroni's multiple comparison test) represent significant differences compared to the control situation.

1966; Chang and Lee, 1977); these calculations took into consideration a mouse average weight of 30 g and a total blood volume of 6% of the body weight.

Isolated CB (20 μg/mL), the basic PLA_2 subunit of CTX, also caused a progressive decline in the amplitude of nerve-evoked skeletal muscle twitches (Fig. 2B), but this effect took a longer time (60 min) to became significant ($p < 0.001$; Fig. 2B) compared to the effect of CTX (Fig. 2A). Unlike CTX (5–20 μg/mL), CB (20 μg/mL) did not cause complete muscle paralysis within the 120 min time-frame of our experiments (Fig. 2B). CB (20 μg/mL) was less potent than the complete venom toxin, CTX (20 μg/mL), which also includes the non-toxic CA subunit. Under the present experimental conditions, CB (20 μg/mL) demanded a longer ($p < 0.0001$) time period (89.85 ± 8.81 min, n = 5) than CTX (20 μg/mL, 43.90 ± 5.20 min, n = 4) to decrease by a half the amplitude of nerve-evoked muscle twitches (Fig. 2A and B).

3.2. Effects of CTX and CB on transmitter exocytosis evoked by phrenic nerve stimulation delivered at 0.2-Hz frequency

We used video-microscopy to monitor real-time transmitter exocytosis from synaptic vesicles of phrenic motor nerve terminals loaded with the FM4-64 fluorescent dye. Both, CTX (5 μg/mL, Fig. 3) and CB (20 μg/mL, Fig. 4), caused biphasic effects on nerve-evoked transmitter exocytosis visualized by the unloading (fluorescence destaining) of synaptic vesicles containing the FM4-64 dye. CTX (5 μg/mL, Fig. 3) and CB (20 μg/mL, Fig. 4) progressively increased (by about 30%) the rate of FM4-64 destaining during 150 s of repetitive electrical nerve stimulation (0.2 Hz-trains, 30 pulses); transient increases in transmitter exocytosis were maximal 20 min after starting incubation with each toxin and their effects only became significant ($p < 0.05$) 120 s after initiating phrenic nerve stimulation. Transmitter release facilitation caused by both CTX and CB declined thereafter, so that nerve-stimulation evoked FM4-64 destaining was similar when comparing the control situation with CTX (5 μg/mL, Fig. 3) or CB (20 μg/mL, Fig. 4) incubated for 54 min. Full decline of transmitter exocytosis detected as an absence of FM4-64 destaining during repetitive electrical stimulation of phrenic nerve was only observed 90 min after starting incubation with CTX (5 μg/mL, Fig. 3) and CB (20 μg/mL, Fig. 4); under these conditions, CTX (5 μg/mL, Fig. 3) and CB (20 μg/mL, Fig. 4) reduced the FM4-64 fluorescence decay at the nerve terminal region by 97 ± 9% and 92 ± 7%, respectively, 150 s after starting the phrenic nerve stimulation. It is worth to note that immediately before the onset of stimulation periods (0, 4, 20, 54 and 90 min), each motor nerve terminal still exhibited FM4-64 fluorescently loaded synaptic vesicles (see Materials and methods), strengthening our contention that CTX and CB directly interfere with transmitter exocytosis.

3.3. Effects of CTX and CB on [^{3}H]ACh release and myographic recordings caused by phrenic nerve stimulation with 5-Hz frequency trains

Fig. 5A shows that CTX (5 μg/mL) and CB (20 μg/mL) time-dependently decreased [^{3}H]ACh release from phrenic nerve terminals stimulated supramaximally with 5-Hz trains. In control conditions the S_2/S_1 and S_3/S_1 ratios were 0.83 ± 0.05 (n = 6) and 0.84 ± 0.06 (n = 6), respectively. Pre-incubation with CTX (5 μg/mL) or CB (20 μg/mL), applied for 18 min before S_2, did not significantly ($p > 0.05$) change the S_2/S_1 ratio compared to the control situation (Fig. 5A, left graph). However, the S_3/S_1 ratio decreased to 0.33 ± 0.04 (n = 5) and 0.26 ± 0.07 (n = 5) when innervated hemidiaphragm preparations were exposed during 54 min with CTX (5 μg/mL) and CB (20 μg/mL), respectively (Fig. 5A, right graph). These results indicate that both toxins reduced the release of [^{3}H]ACh from stimulated phrenic nerve endings by about 60–70%.

These radiochemical experiments were compared with myographic recordings using the same paradigm to stimulate the phrenic nerve (Fig. 5B). In control conditions, the amplitude of nerve-evoked muscle twitches induced by 5-Hz stimulation trains did not change significantly with time, i.e. the S_2/S_1 and S_3/S_1 ratios were 0.95 ± 0.02 (n = 4) and 0.95 ± 0.03 (n = 4), respectively. Pre-incubation with CTX (5 μg/mL, for 18 min before the S_2) caused a small increase in the S_2/S_1 ratio (1.04 ± 0.02, n = 4) compared to the control situation (Fig. 5B, left graph). This situation was totally reversed by prolonging to 54 min the exposure time period of the preparations to CTX (5 μg/mL); under these conditions, CTX (5 μg/mL) decreased by 40% ($p < 0.05$) the amplitude of muscle twitches accounting for a reduction of the S_3/S_1 ratio to 0.56 ± 0.11 (n = 4) (Fig. 5B, right graph). The CB subunit (20 μg/mL) failed to affect ($p > 0.05$) the amplitude of skeletal muscle twitches evoked by phrenic nerve stimulation with 5-Hz frequency trains, i.e. the

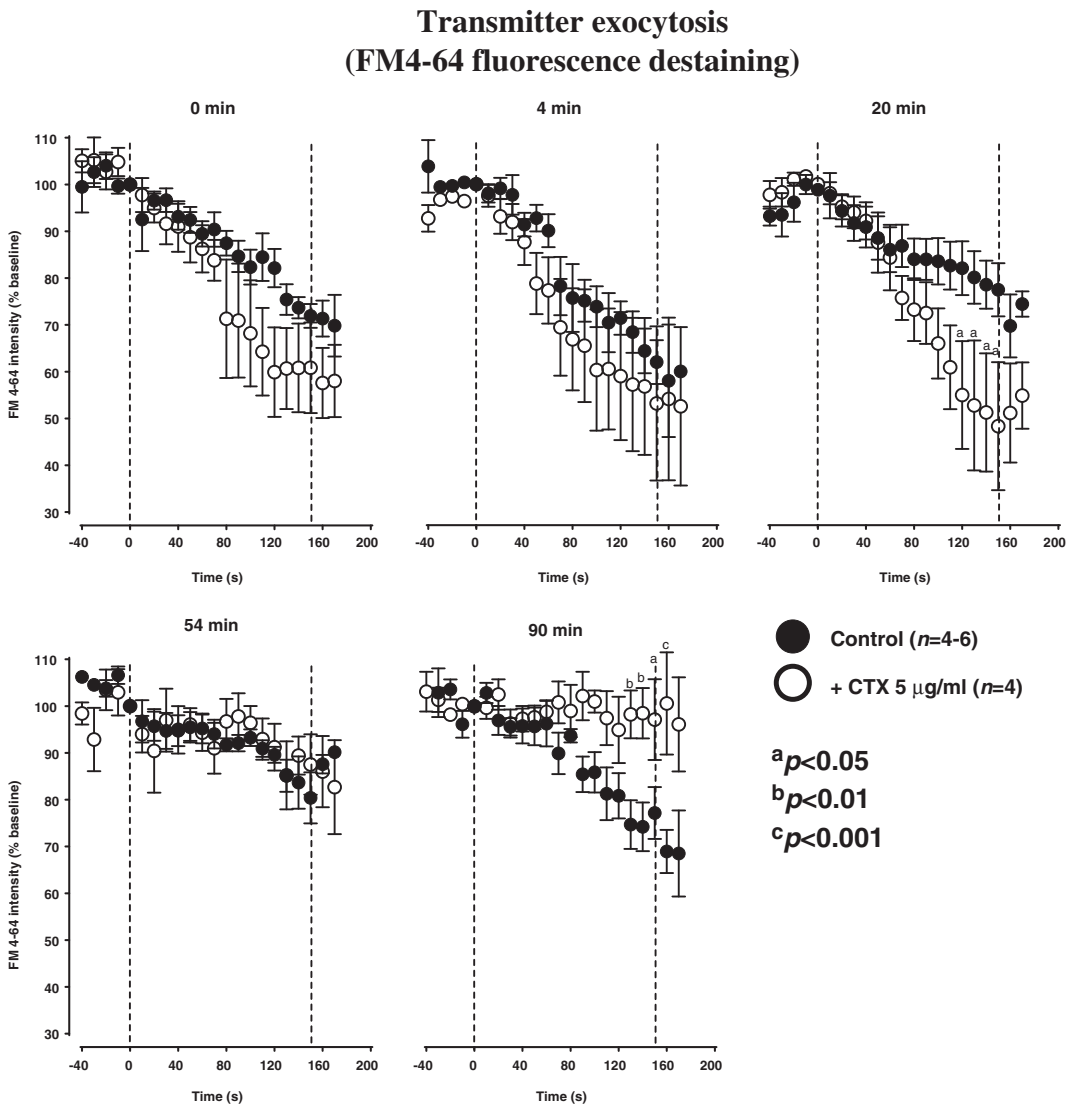

Fig. 3. Nerve-evoked transmitter exocytosis measured by video-microscopy using the FM4-64 fluorescent dye on mice hemidiaphragm preparations exposed to CTX for 0, 4, 20, 54 and 90 min. Graphs show the FM4-64 decay during electrical stimulation of the phrenic nerve (0.2 Hz, 0.5 ms, 30 pulses) in the absence (control) and in the presence of CTX (5 µg/mL). Vertical dashed lines represent the beginning and the end of the stimulation period. Fluorescence decay is expressed as a percentage of maximal dye loading considering that 100% is the fluorescence intensity at zero time. n represents the number of independent experiments. The vertical bars represent ± SEM. $^{a}p < 0.05$, $^{b}p < 0.01$ and $^{c}p < 0.001$ (multiple *t*-test assuming the same scatter per point, Bonferroni-Dunn method) represent significant differences compared to the control situation.

S_2/S_1 and S_3/S_1 ratios observed in the presence of CB (20 µg/mL) were 0.97 ± 0.01 (n = 4) and 0.84 ± 0.05 (n = 4) when the preparations were exposed to the toxin for 18 and 54 min, respectively (Fig. 5B).

4. Discussion

The neurotoxic activity of CTX from *Crotalus durissus terrificus* venom has been attributed mainly to the inhibition of neurotransmitter release by motor nerve terminals (Chang and Lee, 1977; Hawgood and Smith, 1977; Hawgood and Santana de Sa, 1979; Su and Chang, 1984). Notwithstanding this, a postsynaptic action on muscle-type nicotinic receptors has also been ascribed to this toxin (Brazil et al., 1966, 2000; Bon et al., 1979). In this study, we investigated the presynaptic activity of CTX and of its isolated basic PLA_2 subunit, CB, on mice phrenic nerve diaphragm preparations by real-time fluorescence video-microscopy and radiolabelled ACh release techniques. These approaches allowed us to investigate the influence of both CTX and CB on transmitter exocytosis without the influence of the postsynaptic component, which constitutes an add-on to the results obtained previously using electrophysiology recordings with sharp microelectrodes relying on muscle action potentials generation in conditions where the safety margin of the neuromuscular transmission was necessarily decreased. The kinetics of toxin-induced neuromuscular blockade was also investigated measuring the amplitude of evoked myographic contractions using two different neurostimulation patterns, 0.2 Hz twitches and 5 Hz trains, respectively.

Nerve-evoked myographic recordings showed that CTX, applied in a concentration (5 µg/mL) that is 3–6 fold higher the estimated blood concentration of an intravenous LD_{50} of the toxin (Brazil et al., 1966; Chang and Lee, 1977), caused muscle paralysis 90 min after exposure of the preparations when the phrenic nerve was stimulated with supramaximal pulses delivered at 0.2-Hz frequency. The time course of muscle paralysis caused by CTX (5 µg/mL) was not much different from that obtained with higher toxin concentrations (up to 20 µg/mL). Interestingly, CTX (5 µg/mL) increased (by < 10%) the amplitude of muscle twitches compared to the control situation and this was observed within the first 15-min of toxin incubation. In view of its potency, we thought that 5 µg/mL would be the most appropriate concentration of CTX to use in our study. Regarding CB, the basic PLA_2 subunit, a higher concentration (20 µg/mL) was needed in order to

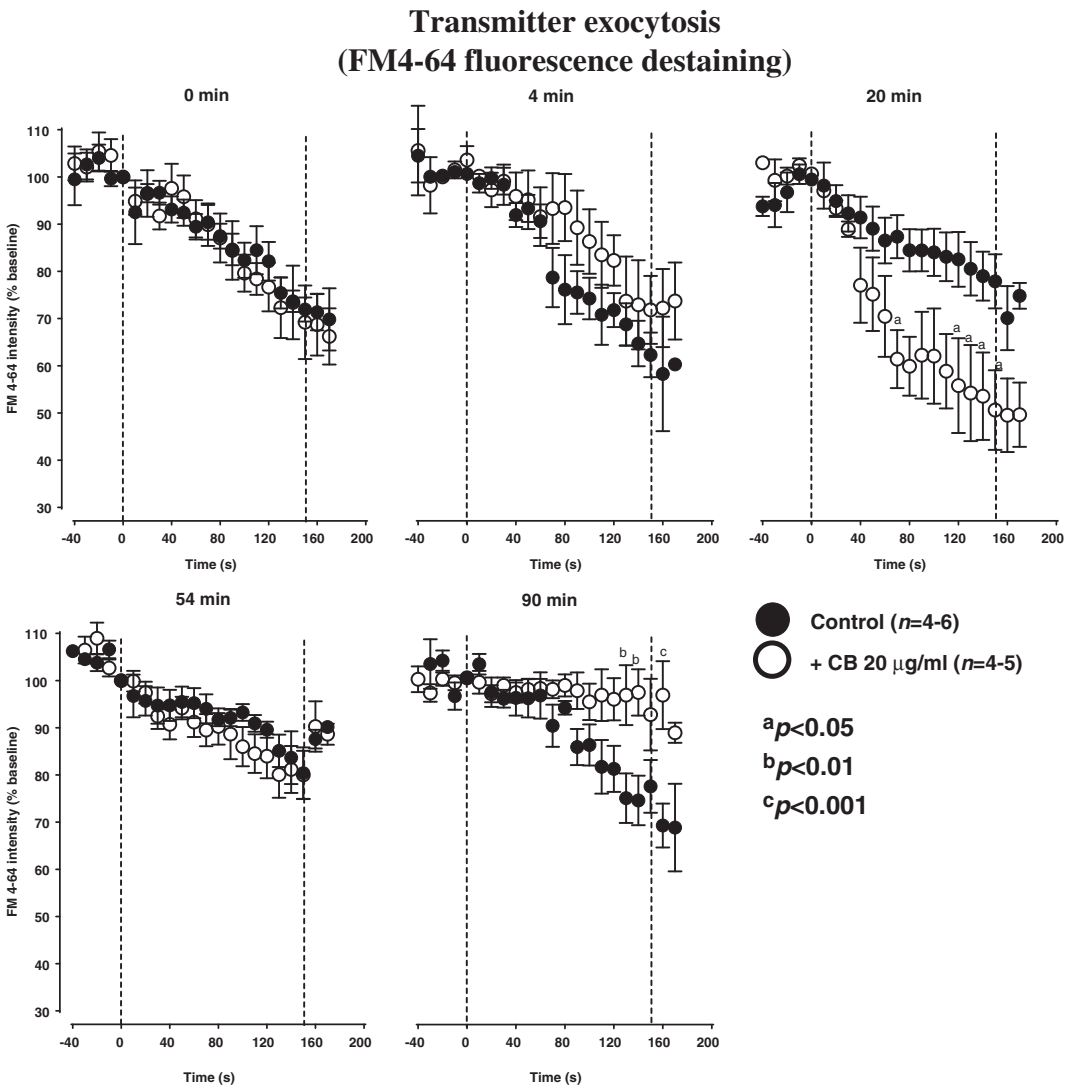

Fig. 4. Nerve-evoked transmitter exocytosis measured by video-microscopy using the FM4-64 fluorescent dye in mice hemi-diaphragm preparations exposed to CB for 0, 4, 20, 54 and 90 min. Graphs show the FM4-64 decay during electrical stimulation of the phrenic nerve (0.2 Hz, 0.5 ms, 30 pulses) in the absence (control) and in the presence of CB (20 μg/mL). Vertical dashed lines represent the beginning and the end of the stimulation period. Fluorescence decay is expressed as a percentage of maximal dye loading considering that 100% is the fluorescence intensity at zero time. n represents the number of independent experiments. The vertical bars represent ± SEM. $^{a}p < 0.05$, $^{b}p < 0.01$ and $^{c}p < 0.001$ (multiple *t*-test assuming the same scatter per point, Bonferroni-Dunn method) represent significant differences compared to the control situation.

obtain a comparable neuromuscular blocking effect to CTX (5 μg/mL). This may happen because in the absence of its CA chaperone, CB tends to bind to non-specific sites, which decreases its effectiveness (Bon et al., 1979; Délot and Bon, 1993). Another possible explanation may be that CB, in the absence of its chaperone CA, binds preferentially to the presynaptic nerve terminal lacking the postsynaptic blocking component required to increase its paralytic potency on nerve-evoked muscle twitches. This hypothesis will be discussed in the following paragraphs.

The biphasic effect of CTX (5 μg/mL) was confirmed by real-time video-microscopy using the FM4-64 fluorescent dye to measure transmitter exocytosis from mice isolated hemidiaphragm preparations stimulated indirectly via the phrenic nerve trunk at 0.2-Hz frequency. The isolated CB (20 μg/mL) subunit reproduced the biphasic effect of CTX (5 μg/mL) on evoked transmitter release. Both CTX (5 μg/mL) and CB (20 μg/mL) increased transmitter exocytosis during the first 20 min of application, but release facilitation declined thereafter and nerve-evoked transmitter release was abolished 90 min after starting application of the toxins. These findings are in agreement with previous electrophysiological studies showing complex initial transitory effects of both CTX and CB on the nerve-evoked quantal release of ACh; both depression and/or facilitation may occur depending on the experimental conditions, yet regardless of the initial events endplate potentials (EPPs) eventually become fully depressed (Brazil and Excell, 1971; Chang and Lee, 1977; Hawgood and Santana de Sa, 1979; Chang and Su, 1982; Su and Chang, 1984). Although electrophysiological studies have been crucial to demonstrate the presynaptic effect of CTX and CB, they are based on indirect evaluations of neurotransmitter release through the depolarization caused by ACh released at the motor endplate. In order to make an accurate estimate of EPPs, the muscle fiber action potentials must be abolished and the experimental procedures used with this aim often interfere with the transmitter release process (Wood and Slater, 2001; Faria et al., 2003). Therefore, it is noteworthy that the real-time video microscopy technique used in this study has certain advantages upon the electrophysiological methods since it permits the direct observation of the neurotransmitter exocytosis process and it does not rely on the function of the postsynaptic muscle membrane. Hence, the present study shows, for the first time, the effect of CTX and of its basic PLA_2 subunit, CB, directly on the kinetics of transmitter exocytosis under conditions of transmitter release closer to the physiological ones (see below).

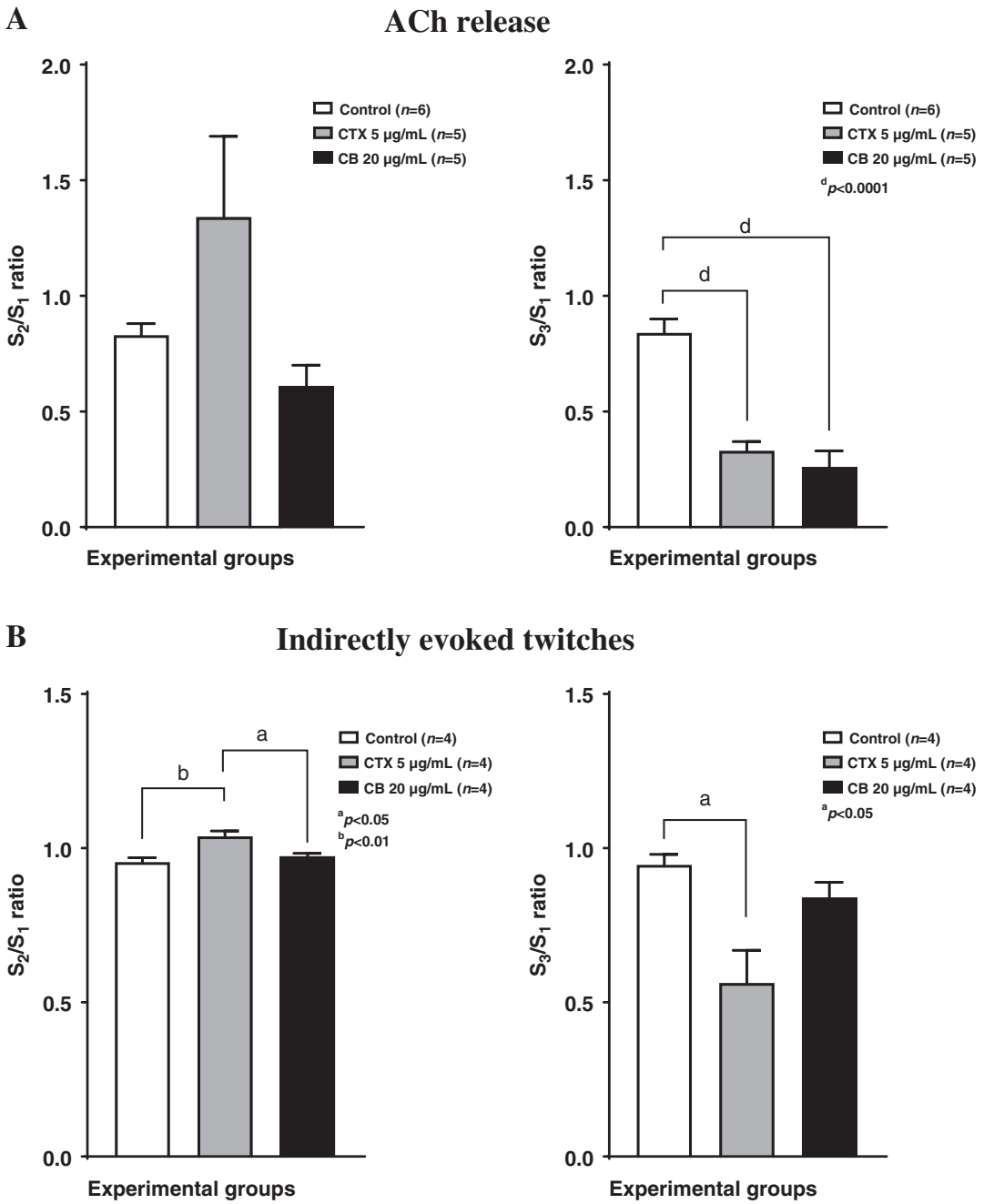

Fig. 5. Effects of CTX (5 µg/mL) and CB (20 µg/mL) on: (A) [^{3}H]ACh release and (B) diaphragm muscle twitches elicited by phrenic nerve stimulation with supramaximal intensity pulses delivered with 5-Hz trains during 2.5 min (750 pulses). Three periods of electrical stimulation, starting at the 12th (S_1), 39th (S_2) and 75th (S_3) min after the end of washout (zero time), were delivered to the phrenic nerve trunk. Changes in the ratio between nerve-evoked [^{3}H]ACh release or muscle twitches during S_2 and S_3 relative to that observed in control conditions, i.e. in the absence of test drugs (S_1), were taken as a measure of the effects of the toxin. The white bars represent S_2/S_1 and S_3/S_1 ratios obtained in the absence of toxins. Results are expressed as mean ± SEM. $^a p < 0.05$, $^b p < 0.01$ and $^d p < 0.0001$ (one-way ANOVA followed by Bonferroni's multiple comparison test) represent significant differences among the groups.

Despite the molecular mechanism underlying the presynaptic effect of CTX is poorly understood, the initial transmitter release facilitation has been attributed to the blockade of slowly activating K^+ channels on motor nerve endings, which may prolong the action potential duration and, thereby, increase the influx of Ca^{2+} through voltage-sensitive channels (Dreyer and Penner, 1987; Rowan and Harvey, 1988). As a consequence, Ca^{2+} influx may promote activation of SNARE proteins favouring the fusion probability of synaptic vesicles with the plasma membrane and, thereby, the transmitter exocytosis. Supporting this hypothesis, recently Lomeo et al. (2014) showed the involvement of Ca^{2+} in the facilitatory effect of CTX on transmitter release in glutamatergic synapses. It is clear that the early facilitatory phase of the CTX effect on transmitter release is not mediated by an enzymatic activity, since inhibition of PLA_2 activity by reducing the temperature, removal of calcium from the extracellular medium and its replacement by strontium were not able to abolish this transient facilitatory phase (Su and Chang, 1984; Rowan and Harvey, 1988; Chang and Lee, 1977; Chang et al., 1977). Thus, although we have shown that CB also promotes a transitory increase of transmitter exocytosis, one may argue that the mechanisms involved in the facilitatory effects of both CTX and CB are independent of the PLA_2 activity. Conversely, the enzymatic activity has been associated with the inhibitory presynaptic effect of

CTX, since it was prevented in experimental conditions designed to inhibit PLA_2 activity (Hawgood and Smith, 1977; Chang and Lee, 1977; Trivedi et al., 1989). In agreement with this hypothesis, we showed that both CTX and CB caused a final decline of ACh exocytosis. Notwithstanding the fact that intrinsic PLA_2 activity of CTX may be necessary for the paralytic action of the toxin, other factors might be involved in the dynamics of the neuromuscular blockage, because higher concentrations of the PLA_2 subunit, CB, were required to produce a similar degree of effect.

Neurochemical studies and myographic recordings, performed under the same experimental conditions, showed that CTX (5 μg/mL) reduced by about 40% the amplitude of nerve-evoked muscle contractions, while decreasing by 60% the release of [^{3}H]ACh triggered by 5-Hz frequency stimulation trains. This discrepancy was exaggerated when testing the effect of its basic subunit (CB) exhibiting PLA_2 activity. CB (20 μg/mL) alone decreased [^{3}H]ACh release from stimulated phrenic nerve endings by a similar extent (69%) as CTX (5 μg/mL), thus supporting the theory that the inhibitory presynaptic action of the toxin depends, in part, on its enzymatic activity. Despite the inhibitory activity of CB (20 μg/mL) on nerve-evoked [^{3}H]ACh release, it was unable to block diaphragm muscle contractions triggered by 5-Hz frequency stimulation trains, a situation that was different from the partial block of the neuromuscular transmission detected during 0.2-Hz twitches.

At this point, it is important to note that the transmission of signals from nerve to muscle is an extremely reliable process, occurring even when the amount of transmitter released per nerve impulse declines substantially, providing that nicotinic receptors at the motor endplate are available to bind released ACh. This feature is mainly because the neuromuscular junction has a high safety margin of synaptic transmission, i.e. the amount of ACh released from stimulated motor nerve terminals normally exceeds the amount of transmitter that is required to bind to muscle-type nicotinic receptors and to excite muscle fibres (reviewed in Wood and Slater, 2001). The output of neurotransmitter from motor nerve terminals may be 4-fold greater than that necessary to evoke a propagated response in every muscle fiber (Paton and Waud, 1967). This means that even if evoked transmitter release lowers by approximately 70% of the control condition, the transmission of the signal to the muscle still occurs in particular during high-frequency neuronal firing such as that occurring in the course of the respiratory drive to the diaphragm in non-anesthetized animals (e.g. Monteiro and Ribeiro, 1987; discussed in Correia-de-Sá et al., 1996; Oliveira et al., 2004). Taking our results together, it appears that depression of transmitter exocytosis caused by CTX is not enough, on its own, to explain paralysis of skeletal muscle fibres in response to electrical stimulation of motoneurons within their physiological firing range. Previous studies have shown that CTX depresses the response of denervated rat diaphragm strips to ACh and, likewise, CTX irreversibly inhibits electric responses of *Electrophorus electricus* electroplaques to cholinergic agonists (Brazil, 1966; Bon et al., 1979). These authors argued that besides its presynaptic inhibitory action, CTX acts postsynaptically by stabilizing the nicotinic receptor conformation in its desensitized form. This theory may explain why CB alone does not promote muscle paralysis, despite having a similar pre-synaptic action to CTX.

In conclusion, we gathered new evidence that CTX inhibitory presynaptic action involves the participation of its basic subunit (CB) with PLA_2 activity on neurotransmitter exocytosis. One may also speculate about the need for CB coupling to its chaperone, CA, in order to exert an effect on postsynaptic nicotinic receptors, which seems to be mandatory to increase the paralytic potency of the CTX heterodimer (cf. Bon et al., 1979; Délot and Bon, 1993). While we understand that the detailed mechanism of action of both CTX and its enzymatic component, CB, remains elusive, important advances on how this toxin complex affects neuromuscular transmission has been achieved with the present study. Notwithstanding the need for better understanding of the biological activity of this toxin in order to improve the treatment of snakebite accidents, data from this study may also be valuable to provide new research tools and therapeutic targets for neuromuscular transmission disorders.

Acknowledgments

This work was partially supported by Fundação de Amparo a Pesquisa do Estado de São Paulo (FAPESP-Brazil 2012/00428-8, 2013/03624-5 and 2013/17864-8), Coordenação de Aperfeiçoamento de Pessoal de Nível Superior (CAPES-Brazil, Toxinology 1592/2011), Conselho Nacional de Desenvolvimento Científico e Tecnológico (CNPq-Brazil, 300596/2013-8). PCS, JBNM and MAT were also supported by Fundação para a Ciência e a Tecnologia (FCT, projects PEst-OE/SAU/UI0215/2014 and UID/BIM/4308/2016) and by the University of Porto/Santander Totta (022015/2015). The authors wish to thank Mrs. Helena Costa e Silva and Belmira Silva for their valuable technical assistance.

Conflict of interest statement

The authors declare there is no conflict of interest.

References

Almeida, C.S., Andrade-Oliveira, V., Camara, N.O., Jacysyn, J.F., Faquim-Mauro, E.L., 2015. Crotoxin from *Crotalus durissus terrificus* is able to down-modulate the acute intestinal inflammation in mice. PLoS One 10, e0121427.

Betz, W.J., Bewick, G.S., Ridge, R.M., 1992. Intracellular movements of fluorescently labeled synaptic vesicles in frog motor nerve terminals during nerve stimulation. Neuron 9, 805–813.

Bon, C., Changeux, J.P., Jeng, T.W., Fraenkel-Conrat, H., 1979. Postsynaptic effects of crotoxin and of its isolated subunits. Eur. J. Biochem. 99, 471–481.

Brazil, O.V., 1966. Pharmacology of crystalline crotoxin. II. Neuromuscular blocking action. Mem. Inst. Butantan 33, 981–992.

Brazil, O.V., Excell, B.J., 1971. Action of crotoxin and crotactin from the venom of *Crotalus durissus terrificus* (South American rattlesnake) on the frog neuromuscular junction. J. Physiol. 212, 34P–35P.

Brazil, O.V., Franceschi, J.P., Waisbich, E., 1966. Pharmacology of crystalline crotoxin. I. Toxicity. Mem. Inst. Butantan 33, 973–980.

Brazil, O.V., Fontana, M.D., Heluany, N.F., 2000. Nature of the postsynaptic action of crotoxin at guinea-pig diaphragm end-plates. J. Nat. Toxins 9, 33–42.

Breithaupt, H., 1976. Enzymatic characteristics of crotalus phospholipase A2 and the crotoxin complex. Toxicon 14, 221–233.

Breithaupt, H., Rubsamen, K., Habermann, E., 1974. Biochemistry and pharmacology of the crotoxin complex. Biochemical analysis of crotapotin and the basic Crotalus phospholipase A. Eur. J. Biochem. 49, 333–345.

Brigatte, P., Faiad, O.J., Ferreira Nocelli, R.C., Landgraf, R.G., Palma, M.S., Cury, Y., Curi, R., Sampaio, S.C., 2016. Walker 256 tumor growth suppression by Crotoxin involves formyl peptide receptors and lipoxin A(4). Mediat. Inflamm. 2016, 2457532.

Chang, C.C., Lee, J.D., 1977. Crotoxin, the neurotoxin of South American rattlesnake venom, is a presynaptic toxin acting like beta-bungarotoxin. Naunyn Schmiedeberg's Arch. Pharmacol. 296, 159–168.

Chang, C.C., Su, M.J., 1982. Presynaptic toxicity of the histidine-modified, phospholipase A2-inactive, beta-bungarotoxin, crotoxin and notexin. Toxicon 20, 895–905.

Chang, C.C., Su, M.J., Lee, J.D., Eaker, D., 1977. Effects of Sr2 + and Mg2 + on the phospholipase A and the presynaptic neuromuscular blocking actions of beta-bungarotoxin, crotoxin and taipoxin. Naunyn Schmiedeberg's Arch. Pharmacol. 299, 155–161.

Correia-de-Sá, P., Sebastião, A.M., Ribeiro, J.A., 1991. Inhibitory and excitatory effects of adenosine receptor agonists on evoked transmitter release from phrenic nerve ending of the rat. Br. J. Pharmacol. 103, 1614–1620.

Correia-de-Sá, P., Timoteo, M.A., Ribeiro, J.A., 1996. Presynaptic A1 inhibitory/A2A facilitatory adenosine receptor activation balance depends on motor nerve stimulation paradigm at the rat hemidiaphragm. J. Neurophysiol. 76, 3910–3919.

Correia-de-Sá, P., Noronha-Matos, J.B., Timoteo, M.A., Ferreirinha, F., Marques, P., Soares, A.M., Carvalho, C., Cavalcante, W.L., Gallacci, M., 2013. Bothropstoxin-I reduces evoked acetylcholine release from rat motor nerve terminals: radiochemical and real-time video-microscopy studies. Toxicon 61, 16–25.

Délot, E., Bon, C., 1993. Model for the interaction of crotoxin, a phospholipase A2 neurotoxin, with presynaptic membranes. Biochemistry 32, 10708–10713.

Dreyer, F., Penner, R., 1987. The actions of presynaptic snake toxins on membrane currents of mouse motor nerve terminals. J. Physiol. 386, 455–463.

Faria, M., Oliveira, L., Timoteo, M.A., Lobo, M.G., Correia-De-Sá, P., 2003. Blockade of neuronal facilitatory nicotinic receptors containing alpha 3 beta 2 subunits contribute to tetanic fade in the rat isolated diaphragm. Synapse 49, 77–88.

Faure, G., Choumet, V., Bouchier, C., Camoin, L., Guillaume, J.L., Monegier, B., Vuilhorgne, M., Bon, C., 1994. The origin of the diversity of crotoxin isoforms in the venom of *Crotalus durissus terrificus*. Eur. J. Biochem. 223, 161–164.

Faure, G., Xu, H., Saul, F.A., 2011. Crystal structure of crotoxin reveals key residues involved in the stability and toxicity of this potent heterodimeric beta-neurotoxin. J. Mol. Biol. 412, 176–191.

Faure, G., Bakouh, N., Lourdel, S., Odolczyk, N., Premchandar, A., Servel, N., Hatton, A., Ostrowski, M.K., Xu, H., Saul, F.A., Moquereau, C., Bitam, S., Pranke, I., Planelles, G., Teulon, J., Herrmann, H., Roldan, A., Zielenkiewicz, P., Dadlez, M., Lukacs, G.L., Sermet-Gaudelus, I., Ollero, M., Corringer, P.J., Edelman, A., 2016. Rattlesnake phospholipase A2 increases CFTR-chloride channel current and corrects F508CFTR dysfunction: impact in cystic fibrosis. J. Mol. Biol. 428, 2898–2915.

Favoretto, B.C., Ricardi, R., Silva, S.R., Jacysyn, J.F., Fernandes, I., Takehara, H.A., Faquim-Mauro, E.L., 2011. Immunomodulatory effects of crotoxin isolated from *Crotalus durissus terrificus* venom in mice immunised with human serum albumin. Toxicon 57, 600–607.

Fernandes, C.A., Pazin, W.M., Dreyer, T.R., Bicev, R.N., Cavalcante, W.L., Fortes-Dias, C.L., Ito, A.S., Oliveira, C.L., Fernandez, R.M., Fontes, M.R., 2017. Biophysical studies suggest a new structural arrangement of crotoxin and provide insights into its toxic mechanism. Sci. Rep. 7, 43885.

Han, R., Liang, H., Qin, Z.H., Liu, C.Y., 2014. Crotoxin induces apoptosis and autophagy in human lung carcinoma cells in vitro via activation of the p38MAPK signaling pathway. Acta Pharmacol. Sin. 35, 1323–1332.

Hawgood, B.J., Santana de Sa, S., 1979. Changes in spontaneous and evoked release of transmitter induced by the crotoxin complex and its component phospholipase A2 at the frog neuromuscular junction. Neuroscience 4, 293–303.

Hawgood, B.J., Smith, J.W., 1977. The mode of action at the mouse neuromuscular junction of the phospholipase A-crotapotin complex isolated from venom of the South American rattlesnake. Br. J. Pharmacol. 61, 597–606.

He, J.K., Wu, X.S., Wang, Y., Han, R., Qin, Z.H., Xie, Y., 2013. Growth inhibitory effects and molecular mechanisms of crotoxin treatment in esophageal Eca-109 cells and transplanted tumors in nude mice. Acta Pharmacol. Sin. 34, 295–300.

Hendon, R.A., Fraenkel-Conrat, H., 1971. Biological roles of the two components of crotoxin. Proc. Natl. Acad. Sci. U. S. A. 68, 1560–1563.

Hernandez-Oliveira, S., Toyama, M.H., Toyama, D.O., Marangoni, S., Hyslop, S., Rodrigues-Simioni, L., 2005. Biochemical, pharmacological and structural characterization of a new PLA2 from *Crotalus durissus terrificus* (South American rattlesnake) venom. Protein J. 24, 233–242.

Lomeo, R.S., Goncalves, A.P., da Silva, C.N., de Paula, A.T., Costa Santos, D.O., Fortes-Dias, C.L., Gomes, D.A., de Lima, M.E., 2014. Crotoxin from *Crotalus durissus terrificus* snake venom induces the release of glutamate from cerebrocortical synaptosomes via N and P/Q calcium channels. Toxicon 85, 5–16.

Marchi-Salvador, D.P., Correa, L.C., Magro, A.J., Oliveira, C.Z., Soares, A.M., Fontes, M.R., 2008. Insights into the role of oligomeric state on the biological activities of crotoxin: crystal structure of a tetrameric phospholipase A2 formed by two isoforms of crotoxin B from *Crotalus durissus terrificus* venom. Proteins 72, 883–891.

Monteiro, E.C., Ribeiro, J.A., 1987. Ventilatory effects of adenosine mediated by carotid body chemoreceptors in the rat. Naunyn Schmiedeberg's Arch. Pharmacol. 335, 143–148.

Noronha-Matos, J.B., Correia-de-Sá, P., 2014. Real-time video exocytosis in rat neuromuscular junction: a powerful live cell imaging technique. In: Méndez-Vilas (Ed.), Microscopy Advances. Formatex, pp. 752–760.

Noronha-Matos, J.B., Morais, T., Trigo, D., Timoteo, M.A., Magalhães-Cardoso, M.T., Oliveira, L., Correia-de-Sá, P., 2011. Tetanic failure due to decreased endogenous adenosine A(2A) tonus operating neuronal Ca(v) 1 (L-type) influx in Myasthenia gravis. J. Neurochem. 117, 797–811.

Oliveira, D.G., Toyama, M.H., Novello, J.C., Beriam, L.O., Marangoni, S., 2002. Structural and functional characterization of basic PLA2 isolated from *Crotalus durissus terrificus* venom. J. Protein Chem. 21, 161–168.

Oliveira, L., Timoteo, M.A., Correia-de-Sá, P., 2004. Tetanic depression is overcome by tonic adenosine A(2A) receptor facilitation of L-type Ca(2 +) influx into rat motor nerve terminals. J. Physiol. 560, 157–168.

Oliveira, L., Correia, A., Costa, A.C., Guerra-Gomes, S., Ferreirinha, F., Magalhães-Cardoso, M.T., Vilanova, M., Correia-de-Sá, P., 2015. Deficits in endogenous adenosine formation by ecto-5′-nucleotidase/CD73 impair neuromuscular transmission and immune competence in experimental autoimmune myasthenia gravis. Mediat. Inflamm. 2015, 460610.

Paton, W.D., Waud, D.R., 1967. The margin of safety of neuromuscular transmission. J. Physiol. 191, 59–90.

Perissinotti, P.P., Giugovaz Tropper, B., Uchitel, O.D., 2008. L-type calcium channels are involved in fast endocytosis at the mouse neuromuscular junction. Eur. J. Neurosci. 27, 1333–1344.

Plomp, J.J., van Kempen, G.T., Molenaar, P.C., 1992. Adaptation of quantal content to decreased postsynaptic sensitivity at single endplates in alpha-bungarotoxin-treated rats. J. Physiol. 458, 487–499.

Prakash, Y.S., Miller, S.M., Huang, M., Sieck, G.C., 1996. Morphology of diaphragm neuromuscular junctions on different fibre types. J. Neurocytol. 25, 88–100.

Rowan, E.G., Harvey, A.L., 1988. Potassium channel blocking actions of beta-bungarotoxin and related toxins on mouse and frog motor nerve terminals. Br. J. Pharmacol. 94, 839–847.

Sampaio, S.C., Hyslop, S., Fontes, M.R., Prado-Franceschi, J., Zambelli, V.O., Magro, A.J., Brigatte, P., Gutierrez, V.P., Cury, Y., 2010. Crotoxin: novel activities for a classic beta-neurotoxin. Toxicon 55, 1045–1060.

Slotta, C.H., Fraenkel-Conrat, M., 1938. Purificação e cristalização do veneno da cobra cascavel. 12. Memórias do Instituto de Butantan, pp. 505–513.

Su, M.J., Chang, C.C., 1984. Presynaptic effects of snake venom toxins which have phospholipase A2 activity (beta-bungarotoxin, taipoxin, crotoxin). Toxicon 22, 631–640.

Trivedi, S., Kaiser, I.I., Tanaka, M., Simpson, L.L., 1989. Pharmacologic experiments on the interaction between crotoxin and the mammalian neuromuscular junction. J. Pharmacol. Exp. Ther. 251, 490–496.

Wang, J.H., Xie, Y., Wu, J.C., Han, R., Reid, P.F., Qin, Z.H., He, J.K., 2012. Crotoxin enhances the antitumor activity of gefinitib (Iressa) in SK-MES-1 human lung squamous carcinoma cells. Oncol. Rep. 27, 1341–1347.

Wessler, I., Kilbinger, H., 1986. Release of [3H]-acetylcholine from a modified rat phrenic nerve-hemidiaphragm preparation. Naunyn Schmiedeberg's Arch. Pharmacol. 334, 357–364.

Wood, S.J., Slater, C.R., 2001. Safety factor at the neuromuscular junction. Prog. Neurobiol. 64, 393–429.

Ye, B., Xie, Y., Qin, Z.H., Wu, J.C., Han, R., He, J.K., 2011. Anti-tumor activity of CrTX in human lung adenocarcinoma cell line A549. Acta Pharmacol. Sin. 32, 1397–1401.